High-β Disruption in Tokamaks

W. Park, E. D. Fredrickson, A. Janos, J. Manickam, and W. M. Tang
Princeton Plasma Physics Laboratory, Princeton, New Jersey 08543
(Received 10 May 1995)

Three-dimensional magnetohydrodynamic simulations of high-β plasmas show that toroidally localized high-n ballooning modes can be driven unstable by the local pressure steepening that arises from the evolution of low-n modes. Nonlinearly, the high-n mode becomes even more localized and produces a strong local pressure bulge that destroys the flux surfaces resulting in a thermal quench. The flux surfaces then recover temporarily but now contain large magnetic islands. This scenario is supported by experimental data.

PACS numbers: 52.55.Fa, 52.35.Py, 52.65.Kj

In the record-setting deuterium-tritium discharges in TFTR, performance is limited by magnetohydrodynamic (MHD) activity, the most dangerous type being the major disruption. This event causes the loss of the confined thermal energy during the thermal quench phase and then the loss of plasma current during the current quench phase [1,2]. In the present day large tokamaks, major disruptions usually occur near the β limit. These high-β disruptions can cause substantial damage to the first wall in larger tokamaks like ITER.

In this Letter, we use the nonlinear 3D resistive MHD code, MH3D [3], to study high-β disruptions. First we obtain a 2D toroidally symmetric equilibrium state using the safety factor q and pressure profiles that correspond to a representative experimental case. The case presented here has $q_0 = 0.92$ at the axis, $q_w = 4$ at the boundary, and $\epsilon\beta_p \equiv 8\pi\epsilon \int p\, ds/\mu_o I_t^2 = 0.3$ with the aspect ratio $R/a = 2.9$. From this 2D equilibrium, a linear $n = 1$ mode with a dominant $m = 1$ component is obtained as shown in Fig. 1, which plots the streamlines of the incompressible part of the velocity (m and n are the poloidal and toroidal mode numbers). This ideal mode nonlinearly evolves to a helically distorted 3D equilibrium as shown in Fig. 2. The upper figure shows the equipressure contours at the toroidal angle $\phi = \pi$ and the lower figure at $\phi = 0$. The maximum pressure gradient occurs at the $\phi = 0$ plane where the local steepening of the pressure gradient occurs in the bad curvature region (the outboard region) [4].

The MH3D code was modified to be able to calculate a mixed-n linear eigenmode evolving from such a 3D equilibrium, by explicitly separating the equilibrium state and the perturbation. A rapidly growing linear ideal mode is obtained as shown in Fig. 3, which plots the stream lines (a) on the poloidal plane and (b) on the midplane of the torus. The mode is localized at the peak pressure gradient at the outboard region. Its structure in this region has a well defined local n number (about 9), even though the global mode has a broad spectrum with $m = -1$ to 20 and $n = 5$ to 14. A similar mechanism for this type of linear mode development has been suggested in analytic studies [5–7], and some of the associated features have been experimentally observed [8]. The crucial question that will be investigated in the following deals with the nonlinear development of this toroidally high-n mode; i.e., whether it will cause a disruption, or just cause a local enhancement of dissipation due to its radial localization, or even saturate harmlessly as in the low-n case.

For the nonlinear evolution of the localized mode, we study a case where the q profile is slightly raised from the previous case such that the plasma does not contain a $q = 1$ surface. This is because, with a $q = 1$ surface present, the present resistive MHD model would have evolved the low-n mode through a complete reconnection

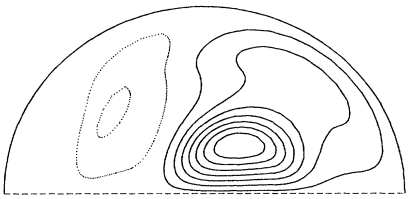

FIG. 1. The streamlines of the linear eigenmode.

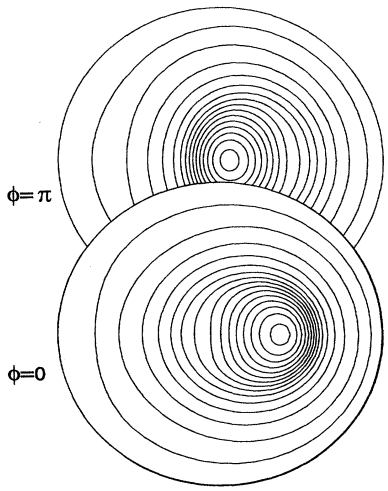

FIG. 2. Pressure contours of the 3D equilibrium.

0031-9007/95/75(9)/1763(4)$06.00

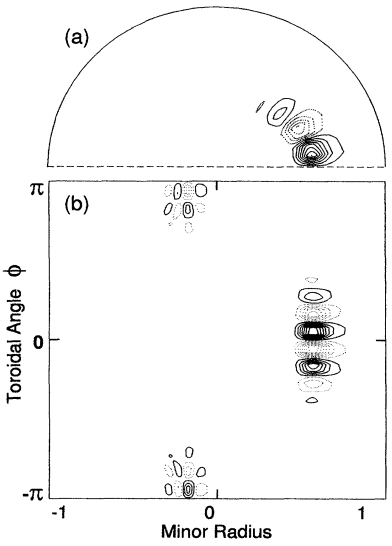

FIG. 3. The streamlines of a mixed n linear eigenmode: (a) on the poloidal plane and (b) on the midplane of the torus.

process instead of the experimentally observed mode saturation. The nonlinear behavior with the present q profile is similar to the experimentally observed trends, which show a saturation of $n = 1$ mode probably due to effects associated with energetic particles [9] and diamagnetic drifts [10]. The present study focuses on the behavior of plasmas with q_0 slightly greater than 1. This is of special interest because the key character of the nonlinear evolution of the high-n mode is an increasing localization, as we will see below, which should not be sensitive to slight changes in the global q values.

Even though q_0 is slightly larger than 1, the linear phase of the calculations yield results similar to the previous case. This is because the mode is driven by the pressure gradient. The nonlinear calculation shows that the steep localized pressure gradient, which gives rise to this toroidally localized high-n mode, becomes even steeper nonlinearly. This causes the nonlinear mode to be increasingly localized, producing a local pressure bulge that strongly pushes into the outer region of plasma as shown in Fig. 4, which plots the temporal evolution of the pressure contours at $\phi = 0$. The local pressure bulge continues to push into the outer region of plasma until it causes most of the plasma region to become stochastic and thereby produce a thermal quench. Figure 5 shows the last phase of Fig. 4 on the midplane of the torus. The fragmentation of pressure contours is due to the fast thermal conduction along the stochastic field lines.

The novel nonlinear behavior just described can be understood from an examination of the linear eigenmode shown in Fig. 3. This fastest growing eigenmode arising from the 3D equilibrium can have either a positive or a negative sign. Since the positive sign gives an outboard

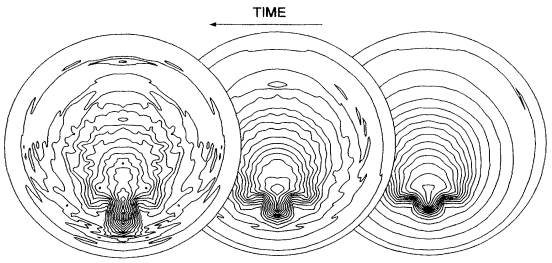

FIG. 4. The nonlinear time development of the pressure.

direction of flow at the position of the local steep pressure gradient, it will further steepen this gradient and make it more localized. This, accordingly, provides a stronger drive to the mode.

There are several ways in which the nonlinearly steepened pressure gradient ultimately relaxes. One path is the thermal quench process just described. Other possible mechanisms include a sawtooth crash, and, to a lesser extent, a fishbone event, where the pressure gradient is flattened in the core region. The pressure gradient can also be relieved without a thermal quench if it touches large neighboring magnetic islands.

Figure 6 shows the theoretical electron cyclotron emission (ECE) signal obtained using a finite amplitude eigenmode from the calculation using the original q profile. The signal is produced by two toroidal rotations with 15 detector sites with the lowest line corresponding to $r = -0.9$ at the inboard region and the uppermost line to $r = 0.9$ at the outboard region. The high-n oscillations are only seen when the underlying $n = 1$ signal is at the maximum phase because this mode is strongly localized toroidally. The calculated signals are in good agreement with the experimental ECE data shown in Fig. 7. Specifically, note that the experimental signal shows similar high-n oscillations superposed on the maximum phase

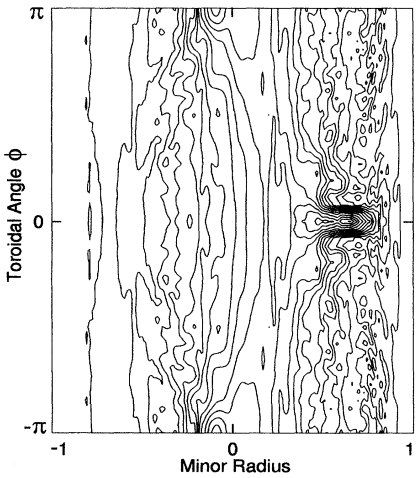

FIG. 5. The pressure contours on the midplane of the torus.

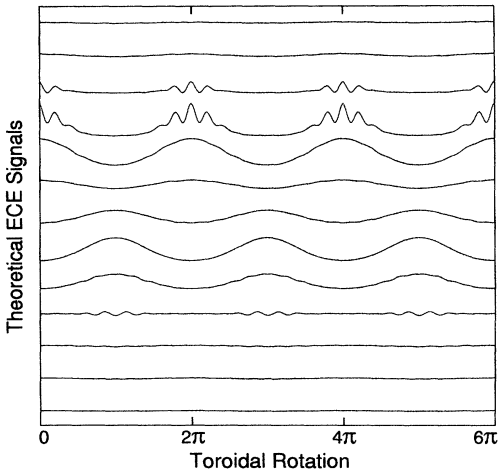

FIG. 6. The theoretical ECE signals.

of the $n = 1$ signal. This confirms that the "bursts" of the high-n mode are actually due to a steadily growing localized high-n mode driven by a nonlinear $n = 1$ distortion. It is only seen when the toroidally localized mode structure comes into view of the ECE detector thereby giving the bursting behavior.

Figure 8 shows the calculated ECE signals from the later two nonlinear states shown in Fig. 4. Only the outboard ECE detector signals are shown. At the later time, the signals clearly indicate that the mode is even more localized and a local pressure bulge is pushing its way toward the boundary. These characteristics are also seen in the experimental ECE data, although this later phase is usually masked by a nonthermal ECE emission.

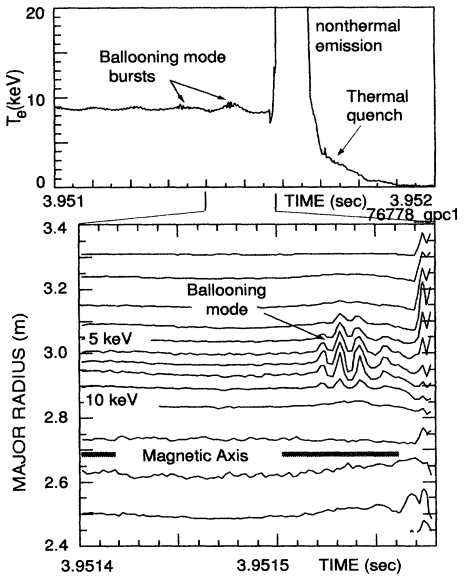

FIG. 7. The experimental ECE signals.

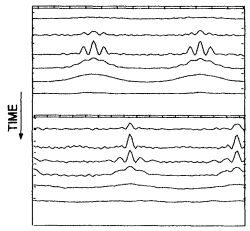

FIG. 8. The calculated ECE signals in the later phase.

These results give additional support to the conclusion that it is the toroidally localized high-n mode and not the low-n mode that causes the thermal quench.

After the thermal quench, a 95% reduction of pressure in the simulation causes the flux surfaces to recover. However, they contain large magnetic islands in the outer region as shown in Fig. 9. (The total pressure loss is usually less than 95%, but the behavior is similar.) This indicates that there exists some pressure confinement in the central region in the post-thermal quench phase. This also agrees with the experimental observation of some pressure recovery in the central region. Such behavior can be understood by the fact that, at small β, the plasma is stable to ideal modes while unstable to resistive modes if the perturbation is large enough. The large perturbation resulting from the thermal quench phase destabilizes the resistive ballooning mode, overcoming layer stabilization effects, such as that described in Glasser, Green, and Johnson [11].

Resistive mode destabilization following a thermal quench, a minor disruption, or a fast-β collapse is a common occurrence not only in TFTR but also in other large tokamaks. In JT-60U, for example, a large $m/n = 2/1$ mode is destabilized right after a fast-β collapse, even though the pressure is much less than pre-β-collapse plasmas where the resistive mode is stable [12]. These trends support the conclusion that the layer stabilization is in effect (overcoming even the neoclassical destabilization) and provides threshold amplitude for the

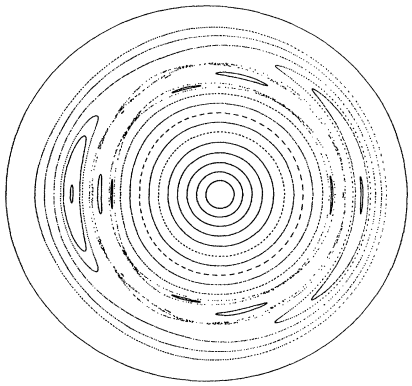

FIG. 9. The reformed flux surfaces.

destabilization of resistive modes. This can also explain whey the good (quiet) discharges in large tokamaks are limited by an ideal mode criterion.

The likely final phase of a major disruption occurs when Z_{eff} becomes high, and the plasma becomes very cold due to line radiation. Since the loop voltage in the experiment is not large enough to sustain the plasma current, the current quench phase sets in to terminate the discharge.

In conclusion, the principal results of this paper can be summarized as follows. As a high-β plasma reaches the ideal mode limit, a low-n mode is first destabilized and the plasma nonlinearly evolves toward a 3D equilibrium containing a localized steep pressure gradient in the bad curvature region. This pressure gradient then drives a new toroidally localized high-n mode. This mode becomes even more localized nonlinearly, producing a local pressure bulge, which strongly pushes into the outer region of the plasma resulting in a thermal quench. When the high-n mode occurs together with sawtooth or fishbone oscillations, it can be less dangerous. After the thermal quench phase, the flux surfaces recover but they contain large magnetic islands. This gives some thermal confinement in the central region and agrees with experimental observations, supporting that a layer stabilization of resistive modes was in effect in the prethermal quench plasma.

Finally, it is appropriate to comment on the other type of high-β disruption that is preceded by a slow-β collapse rather than a thermal quench (fast-β collapse). Although rare in TFTR, this type is more common in other large tokamaks. When the low-n mode does not destabilize the toroidally localized high-n mode, low-n magnetic islands will develop on a resistive time scale resulting in a slow degradation of the confinement. (This can happen, for example, when the low magnetic shear region is small, thereby limiting the saturation amplitude of a low-n mode.) When the outer flux surfaces are finally destroyed, a major disruption will occur.

This work was supported by the United States Department of Energy under Contract No. DE-AC02-76-CHO-3073.

[1] K. McGuire and the TFTR Group, *Plasma Physics and Controlled Nuclear Fusion Research* (IAEA, Vienna, 1986), Vol. 1, p. 421.
[2] E. D. Fredrickson *et al.* (to be published).
[3] W. Park *et al.,* Phys. Fluids B **4**, 2033 (1992).
[4] W. Park *et al.,* Phys. Fluids B **3**, 507 (1991).
[5] M. N. Bussac and R. Pellat, Phys. Rev. Lett. **59**, 2650 (1987).
[6] C. C. Hegna and J. D. Callen, Phys. Fluids B **4**, 3031 (1992).
[7] C. G. Gimblett and R. J. Hastie, Plasma Phys. Controlled Fusion **36**, 1439 (1994).
[8] Y. Nagayama *et al.,* Phys. Fluids B **5**, 2571 (1993).
[9] R. B. White *et al.,* Phys. Rev. Lett. **62**, 539 (1989).
[10] L. Zakharov *et al.,* Phys. Fluids B **5**, 2498 (1993).
[11] A. H. Glasser, J. M. Green, and J. L. Johnson, Phys. Fluids **18**, 875 (1975).
[12] S. Ishida and Y. Kamada (private communication).